Conformational Flexibility in a Staphylococcal Nuclease Mutant K45C from Time-Resolved Resonance Energy Transfer Measurements†

Pengguang Wu‡ and Ludwig Brand*

Department of Biology, Johns Hopkins University, Baltimore, Maryland 21218

Received February 21, 1994; Revised Manuscript Received June 1, 1994®

ABSTRACT: Thermal fluctuations exist in native proteins and other macromolecules in solution. Some may play a role in ligand or receptor binding, control rates of enzymatic catalysis, or define a range of conformations a segment can adopt in solution. We apply the method of time-resolved resonance energy transfer to study the conformational flexibility of a staphylococcal nuclease mutant, K45C, where lysine 45 located at a flexible loop is replaced by a cysteine. We labeled the thiol group with DTNB (5,5′-dithiobis(2-nitrobenzoic acid)) and used the TNB group covalently attached to the protein as an energy acceptor from a single tryptophan at residue 140 as the donor. Conformational flexibility occurring on the time scale of nanoseconds or longer is dispersed as an apparent distance distribution in time-resolved resonance energy transfer measurements. Below room temperature the apparent distance distribution was fitted with a symmetric Lorentzian model with a full width at half maximum height of about 6 Å, indicating substantial degrees of heterogeneity between residues 45 and 140. At room or higher temperature where the protein is in its native state, the apparent distance distribution is asymmetric, indicating the presence of static disorders. Segments in the protein that contribute to the static disorder can be converted to mobile ones with the addition of denaturing guanidinium chloride.

Molecules in solution are subject to thermal fluctuation in conformation. Large molecules such as proteins exhibit various degrees of conformational flexibility (Anfinsen & Scheraga, 1975). An increasing number of experiments (recent reviews by Schulz, 1991; Kempner, 1993) demonstrate that protein conformational flexibility is important in enzymatic catalysis (Rasmussen et al., 1992), receptor binding (Chakraborti et al., 1992), protein insertion into membranes (van der Goot et al., 1991), DNA–protein interactions (Clarke et al., 1991; Chasman et al., 1993; Qian et al., 1992), and function of protein chaperone complexes (Landry et al., 1993). Thus, knowledge of protein internal motions provides important clues for the understanding of many biological processes. In addition the study of protein conformational dynamics can also help improve the design of new proteins or enzymes since the flexibility of one segment in a protein defines the range of conformations it can adopt in solution. There are several reported cases (DeGrado et al., 1991) of newly designed proteins where peptides adopt conformations not intended or desired. An important factor is the flexibility of protein segments in solution.

The time scale of protein conformational flexibility or internal motions can range from picoseconds to seconds. This enormous dynamic range makes it extremely difficult for any single technique to disperse the complete spectrum of motions at all times. It is often the case that one technique detects in part the time characteristics of certain motions and in part the average of others. For example, temperature factors in X-ray or proton-exchange rates in NMR are associated with both fast and slow motions. Fluorescence quenching (Eftink, 1991), fluorescence anisotropy (Beechem & Brand, 1985), and order parameters in NMR (Kay et al., 1989; Stone et al., 1992) are sensitive to picosecond and nanosecond motions. While the existence of motions on various time scales has been relatively easy to infer, the amplitude (or the frequency of occurrence) of these motions is less well understood. Here we apply the method of resonance energy transfer (Haas et al., 1975; Stryer, 1978) to study the conformational flexibility of a staphylococcal nuclease mutant K45C, where lysine 45 is replaced by a cysteine. The loop region around residue 45 is disordered base on X-ray data (Loll & Lattman, 1989), and a solution structure of this protein has yet to appear. While the disorder region in the protein crystal is static, it is not clear how it behaves in solution. Thus this protein provides a suitable example for the study of conformational flexibility in small globular proteins in solution.

In a native protein the long-range distance between two sites is fixed if the structure is rigid, and is dynamic if the structure is flexible. Thus the width of a distance distribution between two sites reflects the internal dynamics of the protein. By measuring different pairwise distance distributions, a better picture of protein dynamics can be obtained. In this work, we employ picosecond fluorescence technique to disperse slow intramolecular motions between two sites in K45C in terms of an apparent distance distribution. The questions we wish to address are as follows: (1) how frequent slow interconversions of conformations occur, (2) what the approximate time scales (or rates) are, and (3) how these conformational heterogeneities are perturbed by temperature and guanidinium within the native state. The findings may serve a basis for future modeling of structural dynamics and complement structural knowledge as determined by other methods.

MATERIALS AND METHODS

(a) Preparation and Labeling of K45C. Staphylococcal nuclease mutant K45C was kindly provided by David Shortle (School of Medicine, Johns Hopkins University). Bacterial growth, isolation, and purification of the protein was similar

† Supported by National Institutes of Health Grant GM 11632.

* Author to whom correspondence should be addressed.

‡ Present address: Tularik Inc., 270 E. Grand Ave., South San Francisco, CA 94080.

® Abstract published in *Advance ACS Abstracts,* July 15, 1994.

0006-2960/94/0433-10457$04.50/0

to that of other nuclease mutants as described elsewhere (James et al., 1992). K45C in the free thiol or oxidized disulfide form was dissolved in 0.1 M Tris, 0.05 M NaCl, and 1 mM EDTA at pH 8.0. Reduction of disulfide dimer was achieved by adding 500-fold excess of dithiothreitol (DTT). Excessive DTT was removed by gel filtration. DTNB (5,5′-dithiobis-(2-nitrobenzoic acid)) in 50-fold excess was added to the protein solution. The sample was stirred for 2 h at room temperature in the dark. Unreacted DTNB and released TNB ion were separated from the modified protein by passing through a Pharmacia PD-10 desalting column. The sample was further purified by an HPLC gel filtration column (BioRad SEC 125). The final buffer was 0.05 M sodium sulfate, 0.02 M sodium phosphate, and 1 mM EDTA at pH 6.9. The labeling ratio (number of thiols modified by DTNB per protein molecule) was quantitated as follows. The TNB covalently attached to the protein was released by adding DTT to a final concentration of 5 mM. From the absorbances of the protein at 280 nm and of TNB at 280 nm as well as 412 nm, the ratio of TNB per protein was calculated to be 1.0. The molar absorbance coefficient of K45C at 280 nm was 15770 M^{-1} cm^{-1}. The absorption coefficient of TNB ion was taken as 14150 M^{-1} cm^{-1} at 412 nm and $\epsilon_{280}/\epsilon_{412} = 0.18$ was used (Riddles et al., 1979). With a slightly lower molar absorption coefficient 13600 at 412 nm (Ellman, 1959), the labeling ratio was 1.04.

(b) Steady-State Fluorescence Measurements. Steady-state fluorescence experiments were performed on an SLM 8000 photon counting spectrophotometer. The thermal denaturation of K45C was monitored by the fluorescence intensity of tryptophan 140 in K45C as a function of temperature. A temperature probe (3-wire platinum) was immersed in the cuvette solution which was stirred by a magnetic stirrer. A transmitter (D1411, Omega Engineering, Inc.) transferred the temperature readings to a PC computer via an RS-232 interface. The scan rate in temperature was about 1 °C/min. Up and down scan in temperature showed the thermal denaturation of K45C was reversible in the concentration range of 20–40 μg/mL. At selected temperatures the total intensities and corrected emission spectra of tryptophan in K45C were collected.

Guanidinium chloride denaturation of K45C was performed at 20 °C. As in the case of temperature denaturation, total intensities and corrected spectra of tryptophan at selected GuHCl concentrations were recorded for subsequent evaluations of Förster distances. The quantum yields of tryptophan 140 in K45C were calculated in reference to free tryptophan which has a quantum yield of 0.14 in water at 25 °C (Eisinger, 1969). Förster distances R_0 at a certain temperature or GuHCl concentration were calculated from the following equation (Förster, 1965)

$$R_0^6 = 8.78 \times 10^{-5} \frac{\phi \kappa^2}{\eta^4} \int F_D(\lambda) \epsilon_A(\lambda) \lambda^4 \, d\lambda$$

where ϕ is the quantum yield of the donor, η, the index of refraction (1.4), F_D, the corrected and normalized emission of donor, ϵ_A, the molar absorption coefficient of acceptor, and κ^2, the orientation factor between donor and acceptor and a dynamic average $^2/_3$ was used.

(c) Time-Resolved Fluorescence Measurements. Fluorescence intensity decays of tryptophan in K45C and K45C–TNB were measured with a picosecond synch-pumped, mode-locked, and cavity-dumped dye laser system and a time-correlated single photon counting apparatus as described earlier (Wu et al., 1991). The overall instrument response was about 60 ps. The excitation wavelength was set at 295 nm and the emission was detected at 350 nm with an emission polarizer at the magic angle 54.7°. A dilute Ludox scattering solution was used to obtain the instrument response. Duplicate or triplicate data sets were collected. Sample cuvette holders were thermostated at various temperatures.

(d) Data Analysis. The decay of donor tryptophan in K45C was analyzed according to a sum of exponentials

$$I_D(t) = \sum \alpha_i \exp(-t/\tau_i) \quad (1)$$

where α_i and τ_i are amplitude and lifetime of component i. For each data set, which contained about 2000 data points, α_i and τ_i were optimized by a nonlinear least-squares method and were used as inputs in the subsequent distance distribution analysis. Effects of temperature and GuHCl concentrations were taken into account.

The donor decay in the presence of acceptor TNB was analyzed by an apparent distance distribution $p(r)$

$$I_{DA}(t) \sum \alpha_i \int p(r) \exp\left[-\frac{t}{\tau_i}\left(1 + \left(\frac{R_0}{r}\right)^6\right)\right] dr \quad (2)$$

Since the energy transfer rate depends both on donor–acceptor distance and on their mutual orientation (Förster, 1965), eq 2 is the sum of transfer rates with donor and acceptor at different distances and orientations. The contribution from orientation is by convention grouped into R_0, which is calculated using a dynamically-averaged value of $^2/_3$ for the orientation factor. When the rotational diffusion rates of donor and acceptor are much faster than the transfer rates, $p(r)$ represents a real distance distribution; when the motions of donor and acceptor are comparable with or slower than the transfer rates, $p(r)$ may contain contributions from distance as well as orientation distributions. Motions on the time scale of picoseconds to the lower nanoseconds tend to average out or narrow down a distribution. Thus the apparent distance distribution obtained by data analysis is due to conformational heterogeneity originating from large amplitude motions wth time scales longer than those of fluorescence decays.

The apparent distance distribution was modeled by either a Gaussian

$$p(r) = \frac{1}{\sqrt{2\pi}\sigma} \exp[-(r - \bar{r})^2/2\sigma^2]$$

or a Lorentzian

$$p(r) = \frac{1}{\pi\sigma}\left[1 + \left(\frac{r - \bar{r}}{\sigma}\right)^2\right]^{-1}$$

where $\bar{r}$ is the mean distance and σ, the standard deviation of the distribution. When necessary, asymmetric distance distribution functions were used where the left half and the right half of the distribution were set unequal (Wu & Brand, 1992).

RESULTS

(a) Stability and Labeling of K45C. Figure 1 shows thermal and GuHCl denaturation profiles of staphylococcal nuclease mutant K45C. They are about the same as those of the wild-type nuclease. This is expected since the flexible loop around residue 45 is not tightly coupled to the overall structure and substitution of one residue does not affect the overall stability of the protein. The transitions appear to be two state, similar to those of wild type and other mutant proteins (Shortle et al., 1988). The change in the fluorescence intensity of a single tryptophan at position 140 in the nuclease mutant protein

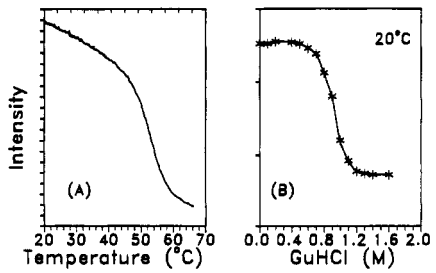

FIGURE 1: Denaturation of K45C. (A) Fluorescence intensity of tryptophan 140 in K45C as a function of temperature. The heating rate was about 1 °C/min. (B) tryptophan intensity as a function of guanidinium concentration. The temperature was at 20 °C. In both A and B the excitation wavelength was at 295 nm and the emission wavelength was at 350 nm.

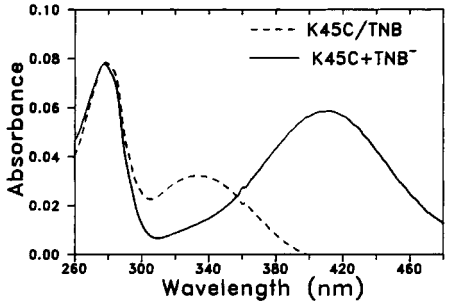

FIGURE 2: Characterization of the labeled protein. Absorption spectrum of K45C with TNB covalently attached to the protein (dashed line). The TNB was released by adding dithiothreitol to 5 mM. The solid line shows the absorption due to TNB ion only (above 300 nm) and TNB ion plus protein around 280 nm.

follows the breakdown of the protein structure as measured by circular dichroism, similar to that of the wild type (Anfinsen et al., 1972) and of other nuclease mutants (Shortle & Meeker, 1986). The denaturation curves in Figure 1 provide reference points in the data analysis of conformational flexibility in this mutant protein in its native and denatured states.

DTNB (Ellman, 1959) is a very useful reagent in the quantitation of thiol groups in proteins. We recently adapted it as an energy acceptor with tryptophan as the donor (Wu & Brand, 1992). DTNB is nonfluorescent in nature but has some compelling advantages as an energy transfer acceptor. The reaction of DTNB with the thiol group is through disulfide exchange (Ellman, 1959) and is therefore site specific. The reaction is reversible and 100% labeling is readily achieved. The chromophore is directly attached to the thiol group, thus eliminating extra linker arms typically associated with modification reagents. Time-dependent heterogeneity introduced by these linker arms can complicate data interpretation substantially, leading to wide apparent distance distributions (Lakowicz et al., 1988; James et al., 1992). Figure 2 shows the absorption spectra of TNB covalently attached to K45C, and free TNB ion plus K45C after DTT was added. TNB covalently attached to K45C has an absorption maximum around 330 nm and thus its absorption overlaps the emission spectrum of tryptophan. The Förster distance, R_0, calculated from the quantum yield of tryptophan in K45C and the overlap integral between the tryptophan emission and TNB absorption is 24.5 Å at 20 °C in the native state. R_0 is slightly higher at lower temperature and lower at higher temperature and in denaturing GuHCl. The variations in R_0 were taken into account in the data analysis.

The quantitative extent of labeling was obtained by adding DTT to release TNB into solution. The ionized form of TNB has an absorption maximum at 412 nm. Use of the known molar absorption coefficient of TNB gave exactly one TNB per protein molecule. The buffer was kept at pH 6.9 to prevent

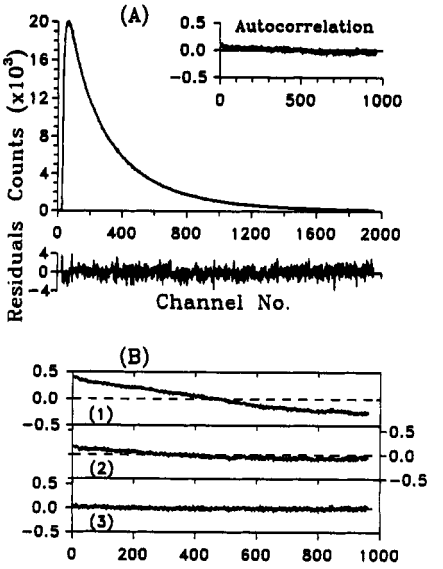

FIGURE 3: (A) Tryptophan fluorescence intensity (counts) in K45C–TNB vs time as channel no. (11 ps per channel). Both measured and fitted curves are plotted. The data were collected at 5 °C and were analyzed by one symmetric Lorentzian apparent distance distribution. The differences between experimental and fitted data are plotted as weighted residuals. The autocorrelation of the residuals is shown in the inset. (B) Autocorrelations of residuals with Gaussian models. The same experimental data were used. (Trace 1) one symmetric Gaussian distance distribution fit. (Trace 2) one asymmetric Gaussian fit. (Trace 3) two symmetric Gaussian fit.

hydrolysis of the label. All samples were kept frozen in the dark prior to the experiments.

(b) Conformational Flexibility in K45C at Low Solution Temperature. We address the issue of conformational flexibility in K45C in its native state by measuring the distance distribution between tryptophan 140 and TNB at residue 45. We analyzed the fluorescence decay of tryptophan in K45C using eq 2. The fit at 5 °C is shown in Figure 3A. We used reduced-χ^2, weighted residuals (difference between measured and fit data), and autocorrelation of the residuals to judge the quality of fit. Since a large number of data points are collected in a single data set in time-resolved single photon counting measurements, correlations among residuals are easily detected when a fit is not adequate. This provides a very sensitive way to judge a fit besides the reduced-χ^2. For all the results in the following, the reduced-χ^2s of fit without systematic deviations in the autocorrelations were within 1.0–1.2. In Figure 3A, one symmetric Lorentzian distance distribution is adequate as indicated by flat residuals and autocorrelation of the residuals.

Like any other parametrized model fitting in data analysis, different models may fit experimental data equally well though some may be meaningless. We tested this by using a different model function. We tried a Gaussian distance distribution and the results are shown in Figure 3B in terms of autocorrelations of the weighted residuals. With one symmetric Gaussian distance distribution the fit was very poor (the corresponding reduced-χ^2 is also high). Attempts to use a skewed Gaussian function improved the fit but not to the degree of satisfaction. With two symmetric Gaussian functions, the results were good as judged by the random distribution of autocorrelation of the residuals.

Thus we can fit the apparent distance distribution between tryptophan 140 and TNB at residue 45 with either one Lorentzian function or two Gaussian functions. A question that naturally arises is: are they significantly different? Figure 4 shows the profile of one Lorentzian distance distribution and that of the superposition of two Gaussian distance

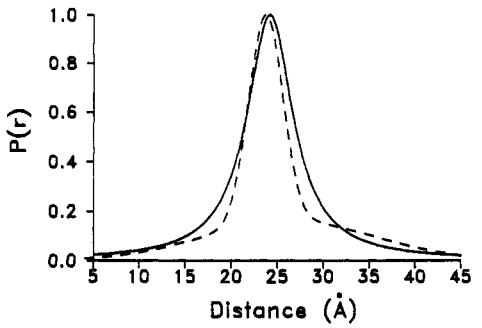

FIGURE 4: Apparent distance distribution between tryptophan 140 and TNB at residue 45 in K45C. The solid line is the profile from one Lorentzian distance distribution fit as shown in Figure 4A. The dashed line is the profile from the superposition of two Gaussian fits as shown in Figure 4B trace 3. Solution temperature was 5 °C.

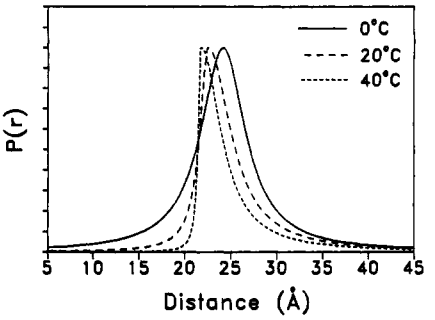

FIGURE 5: Apparent distance distribution between tryptophan 140 and TNB at residue 45 in K45C as a function of temperature. Results at 5 °C were shown in Figure 4. The apparent distance distributions were fitted with symmetric functions at lower temperatures and asymmetric ones at room or higher temperatures.

distributions. Although the functional forms of the two models are quite different, the final results of the fits are very similar. Since a model with two Gaussian functions contains twice as many fitting parameters as one Lorentzian function, we choose a Lorentzian function in the data analysis of the protein in the native state. Thus even though we are not analyzing our data in a "model free" approach, the similarity in the shape of distance distribution from different fitting functions indicates that the Lorentizan model adequately represents the real heterogeneity in the system.

The apparent distance distribution in Figure 4 has a full width at half-maximum height of distribution about 6 Å. This indicates a substantial degree of conformational heterogeneity. Due to the nature of a Lorentzian distribution, the population that falls beyond the half width at either end of the distribution is large. Experimentally, the population below 15 Å is unreliable due to the high degree of quenching of donor fluorescence by the acceptor. The population above 35 Å is likely due to some donor–acceptor orientations with little energy transfer. The major portion of the distribution is symmetric with respect to its mean distance, which itself is close to that from X-ray data. We have demonstrated elsewhere (Wu & Brand, 1992) that if an apparent distance distribution is mainly determined by static orientation between donor and acceptor then its shape is skewed to longer apparent distances. The apparent distance distribution in Figure 4 is thus largely due to real distance heterogeneity in K45C. This heterogeneity represents large amplitude disorders and is determined by the energetics of different conformations. Different kinetic barriers, which govern the rates of interconversion, may exist in these conformations. By thermal perturbation we can gain further details on the time scale of the conversions.

(c) Conformational Flexibility as a Function of Temperature. A protein molecule in solution can sustain a certain degree of thermal perturbation before its overall secondary and tertiary structure break down. Within this temperature range a protein molecule remains native but structural fluctuations are expected to increase at elevated temperature. One may think of the fluctuations either in terms of time scale (short, intermediate, or long time motions) or in terms of space (local, intermediate, or large amplitude motions). Structural constraints in the native state dictate that most of the fluctuations occur locally and are short on time scale. However, it is the intermediate or large amplitude motions that may accompany conformational changes in ligand binding, heterogeneity in structural determination, and domain motions in enzymatic action. These large motions occur much less frequently, simply due to their higher energetics. At higher temperatures, the overall spectrum of motions is expected to shift in the direction of fast motions. Here we observe structural fluctuations using nanosecond fluorescence decay. The apparent distance distribution from data analysis consists of contributions from slow motions that can be dispersed in time and from fast motions that average out certain local heterogeneity. The increase in fast motions will be reflected in the decrease in the width of an apparent distance distribution. Ideally the fast motions could be incorporated into data analysis if the nature of these motions were known and they could be modeled. Molecular dynamics simulations extending into the nanosecond time domain with consideration of solvent molecules may be helpful in the coming years. Despite of this, our results provide useful findings for further understanding of conformational flexibility in proteins.

We collected the decay data of tryptophan in K45C–TNB from 0 °C to 40 °C within which the protein is native. At 0 °C and 5 °C, the decays were analyzed by one symmetric Lorentzian function. At 20 °C and 40 °C, a symmetric Lorentzian fit led to systematic deviation in the autocorrelation of the residuals similar to those in traces 1 and 2 of Figure 3B. An asymmetric Lorentzian distance distribution was required to get a satisfactory fit. The degree of asymmetry is higher at 40 °C. The apparent distance distributions at several temperatures are shown in Figure 5. The apparent distance distribution at 0 °C is very close to that at 5 °C. As the temperature increases, the width of the distance distribution decreases slightly due to increased local and fast motions occurring on picosecond or nanosecond time scales. At and above room temperature, there are still substantial degrees of conformational heterogeneity originating partly from static orientational disorders as indicated by the population of longer apparent distances (Wu & Brand, 1992). The presence of contribution from static orientation eliminates the possibility of large-scale diffusive motions between the donor and acceptor on the time scale of energy transfer and can be understood from the fact that the flexible loop is constrained at both ends by other structural elements of the protein. The change in apparent distance distribution is totally reversible in this temperature range. We cooled down one sample from 40 °C to 5 °C and recovered the same symmetric distance distribution. Thus the shape change as a function of temperature reflects conformational changes in the protein within its native state, i.e., the profile of internal motions already present at low temperature shift toward faster time scales while some slower motions begin to register with rising temperature.

The time scale of some of the slow motions (those with time scales longer than nanoseconds and those resulting in the long apparent distances) can be estimated. The donor decay rate is comparable with the energy-transfer rate (with a lifetime of a few nanoseconds). The time scale of internal motions has

Table 1: Averaged Parameters at Different Temperatures[a]

T (°C)	$\langle\tau_D\rangle$ (ns)	$\langle\tau_{DA}\rangle$ (ns)	E%	$\bar{r}$ (Å)
0	6.04	3.00	50.3	25.1
5	5.85	2.88	50.8	25.2
20	5.27	2.72	48.4	25.1
40	4.49	2.44	45.7	24.5
61	1.28	0.97	24.2	22.0

[a] Average lifetime was calculated using $\langle\tau\rangle = \sum_i \alpha_i\tau_i/\sum_j \alpha_j$. Energy transfer efficiency E was calculated from $E = 1 - \langle\tau_{DA}\rangle/\langle\tau_D\rangle$ and average distance $\bar{r}$ from $\bar{r} = R_0(1/E - 1)^{1/6}$.

to be close to that of energy transfer in order to modulate the observed transfer rate (and therefore change the shape of the distance distribution). The temperature dependence of the apparent distance distribution implies that the time scale of part of the slow motions is in the upper nanosecond or lower microsecond range, within which interconversion of conformations occur. The decrease in the apparent distance distribution at higher temperatures does not contradict the notion of greater disorders in the slightly destabilized protein within the native state because the increase in fast motions average out some of the distribution. The long tail in the apparent distance distribution at 40 °C probably reflects the fact that the protein is still in the native state and some of the internal motions are still restricted.

We also measured the decay of tryptophan in K45C–TNB when the protein is totally denatured at 61 °C. There was about 10–20% chemical decomposition of the acceptor (compared with a fresh sample after cooling) so that a quantitative analysis in the distance distribution was difficult. By multiple exponential analysis we obtained average lifetimes which give some indication of the average distance between donor and acceptor. The results together with those at lower temperatures are shown in Table 1. The overall size of the protein remains about the same as the protein is denatured and thus the denatured state is compact.

(d) Conformational Flexibility in the Presence of Guanidinium. The temperature study showed that at or above room temperature the apparent distance distribution is skewed to longer apparent distances. Clearly some structural changes occurred as a result of thermal perturbation. These changes inside the protein are observed as some static disorders revealed by resonance energy transfer measurements between two sites. Besides temperature, other conditions can also perturb the native structure of a protein. We used guanidinium chloride to destabilize K45C to gain some understanding of the factors that affect its conformational flexibility. If the asymmetry of the apparent distance distribution at 20 °C is mainly due to some static disorders inside the protein, then the disordered regions can be converted into slightly mobile ones when the native state is partially destabilized. In addition to a slightly narrower distribution, a more symmetric shape is expected. This is what we observed as shown in Figure 6. At 0.4 M GuHCl where the protein is still native (Figure 1), the shape of the apparent distance distribution of K45C–TNB becomes more symmetric. We further measured distance distributions at GuHCl concentrations where the protein is partially or totally denatured. At 0.7 M GuHCl, the protein begins to denature. The apparent distance distribution is fitted with one Lorentzian (which may be due to a superposition of the native and denatured states). At 1.0 M GuHCl, which is close to the total breakdown of the structure, both a Lorentzian and a Gaussian fit the decay curve. It is possible there are not many constraints left in the protein structure to skew its distance distribution. At 1.2 M GuHCl, the Förster distance (about 19 Å) is further away from the mean distance of

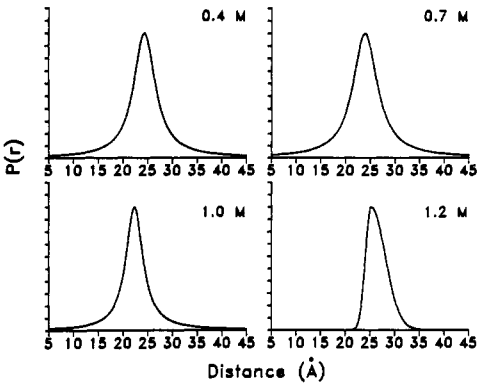

FIGURE 6: Apparent distance distribution as a function of GuHCl at 20 °C. The curve without denaturant was shown in Figure 5. At 0.4 M and 0.7 M GuHCl, only Lorentzian model functions could fit the data. At 1.0 M, both a Gaussian and a Lorentzian could fit the data equally well. Shown in the figure is a Lorentzian fit. A Gaussian fit produced a shape that has a larger half width but a shorter tail. At 1.2 M the mean distance is larger than the Förster distance (about 19 Å) and the shape is less defined from the measurements. We used a Gaussian function in the fit.

distribution and as a result the shape information cannot be rigorously determined. The pertinent information is that the denatured state is quite compact as in the case of another nuclease mutant protein (James et al., 1992).

DISCUSSION

For a structural description of a protein, a set of coordinates of atoms are sufficient to specify the characteristics of the protein. For a complete dynamic description of a protein, these coordinates as a function of time are required. While molecular dynamics simulations follow the motions of individual atoms, they are limited to picoseconds in time course for a protein such as staphylococcal nuclease. Experimentally no methods are available to monitor atoms at all times in solution. Alternatively we can gain insights about the dynamics of proteins by a combination of low resolution but dynamic methods with high-resolution structural methods. In this context, the description of protein dynamics requires three variables: time scale, amplitude, and spatial extent, which have been discussed by McCammon & Harvey (1987). For example, the time scale of motion can range from femtoseconds to longer than seconds, the amplitude can be from 0.01 Å to more than 10 Å, and the spatial extent can be from local to global. In resonance energy transfer measurements detected by time-resolved fluorescence, the time window is on nanoseconds. Dynamic events occurring on the time scale of picoseconds or less lead to averaged signals, those on nanoseconds modulate the detected signals, and those on slower time scales appear static. For example, slow conformational conversions in complex carbohydrate chains have been observed by time-resolved resonance energy transfer methods (Wu et al., 1991), and these transitions cannot be measured by methods with slower signal detection. As for the amplitudes and spatial extents of internal motions, time-resolved resonance energy transfer measurements offer unique advantage. This relies on the fact that for motions slower than nanoseconds the observed decay curve is the superposition but not the average of all possible transfer rates between the donor and acceptor at different distances and orientations. Since resonance energy transfer can occur from 10 Å to 100 Å with appropriate donor–acceptor pairs, large spatial disorder can be studied by this method.

Our results provide some assessment about the amplitudes and time scales of internal motions in the nuclease in solution. The thiol group in staphylococcal nuclease mutant K45C is

located in a flexible loop known from X-ray data of the wild type nuclease (Loll & Lattman, 1989). If a segment shows flexibility in crystal form, the degree of flexibility is expected to be larger in solution. The distance distribution between tryptophan and TNB at residue 45 such as in Figure 4 shows that, viewed from Trp 140, the TNB group attached to Cys 45 can move as much as 10 Å (about 5 Å from either side of the average). These large amplitude motions occur at a time scale longer than nanoseconds. Since the TNB is bound though a disulfide bond to the side chain of Cys 45, the distance distribution should reflect the conformational flexibility of the region, primarily from the flexible loop. It is worthwhile to note that the results from time-resolved resonance energy transfer provides a probability function of the flexibility in solution while the large amplitude conformational changes observed in X-ray studies such as those of calmodulin bound to receptor peptide (Meador et al., 1993) or calcium-bound rat annexin V (Concha et al., 1993) reflect the magnitude and final states of the change.

That the shape of the distribution is not a Gaussian can be understood partially from the viewpoint of coupled motions. If the motion of each individual bond is a Gaussian random process and if each bond moves independent of another, then the overall process is also a Gaussian. A simple Gaussian distance distribution is expected. In proteins, however, the motion of one bond is coupled to that of another one. Even though the motion of each individual bond may be a Gaussian, the overall or collective motion may not be a Gaussian. Thus we have an apparent distance distribution that does not resemble a simple Gaussian. Another factor that may play a role in the observed shape of distance distribution is that the coupled motions are occurring on different time scales and what we observed is the superposition of these motions.

Within the native state of a protein molecule, conformational fluctuation varies with changing thermal or solvent perturbation. As temperature rises, rates of thermal motions increase accordingly and each atom samples more configurations in the protein. Upon a change of temperature from 0 °C to 20 °C (Figure 5), there is a large increase in thermal motion inside K45C. At 40 °C the increase is much higher. Even with enhanced motion the region around 45 loop may still exhibit some long time motions as disorders. This correlates well with the difficulties in resonance assignments of residues surrounding this loop in staphylococcal nuclease in NMR experiments (Torchia et al., 1989). Addition of guanidinium similarly destabilizes the native structure and increases the structural fluctuation. The effects of GuHCl appear to be different from those of temperature, probably reflecting the fact that there may be binding of GuHCl to the protein surface in addition to the change of solvent characteristics.

The use of resonance energy transfer as measured by time-resolved fluorescence methods is valuable in better understanding large amplitude or long time scale motions that may exist in certain parts of a protein. With the development of molecular dynamics extending into longer time domain, the nature of these motions can be better understood. Site-directed mutagenesis provides a powerful means to select different sites in a protein so that domain motions can be investigated in a great detail, providing a deeper understanding of protein structure and function. With knowledge of the amplitude and time scale of slow conformational changes, important molecular mechanisms such as induced fit in antibody–antigen interaction (Rini et al., 1992) may be better understood.

ACKNOWLEDGMENT

We are thankful to Professor David Shortle and Wes. Stites for the gift of the clone of staphylococcal nuclease mutant K45C.

REFERENCES

Anfinsen, C. B., & Scheraga, H. A. (1975) *Adv. Protein Chem. 29*, 205–300.
Anfinsen, C. B., Schechter, A. N., & Taniuchi, H. (1972) *Cold Spring Harbor Symp. Quant. Biol. 36*, 249–55.
Beechem, J. M., & Brand, L. (1985) *Annu. Rev. Biochem. 54*, 43–71.
Charkraborti, P. K., Garabedian, M. J., Yamamoto, K. R., & Simons, S. S., Jr. (1992) *J. Biol. Chem. 267*, 11366–73.
Chasman, D. I., Flaherty, K. M., Sharp, P. A., & Kornberg, R. (1993) *Proc. Natl. Acad. Sci. U.S.A. 90*, 8174–8.
Clarke, N. D., Beamer, L. J., Goldberg, H. R., Berkower, C., & Pabo, C. O. (1991) *Science 254*, 267–70.
Concha, N. O., Head, J. F., Kaetzel, M. A., Dedman, J. R., & Seaton, B. A. (1993) *Science 261*, 1321–4.
DeGrado, W. F., Raleigh, D. P., & Handel, T. (1991) *Curr. Opin. Struct. Biol. 1*, 984–93.
Eftink, M. R. (1991) in *Topics in Fluorescence Spectroscopy. Vol. 2 Principles* (Lakowicz, J. R., Ed.) pp 53–126, Plenum Press, New York.
Eisinger, J. (1969) *Photochem. Photobiol. 9*, 247–58.
Ellman, G. L. (1959) *Arch. Biochem. Biophys. 82*, 70–7.
Förster, T. (1965) in *Modern Quantum Chemistry* (Sinanoglu, O., Ed.) Vol. III, pp 9–137, Academic Press, New York.
Haas, E., Wilchek, M., Katchalski-Katzir, E., & Steinberg, I. Z. (1975) *Proc. Natl. Acad. Sci. U.S.A. 72*, 1807–11.
James, E., Wu, P. G.; Stites, W., & Brand, L. (1992) *Biochemistry 31*, 10217–25.
Kay, L. E., Torchia, D. A., & Bax, A. (1989) *Biochemistry 28*, 8972–9.
Kempner, E. S. (1993) *FEBS Lett. 326*, 4–10.
Lakowicz, J. R., Gryczynski, I., Cheung, H. C., Wong, C. K., Johnson, M. L., & Josh, N. (1988) *Biochemistry 27*, 9149–60.
Landry, S. J., Ryalls, J. Z., Fayet, O., Georgopoulos, C., & Gierasch, L. M. (1993) *Nature 364*, 255–8.
Loll, P. J., & Lattman, E. E. (1989) *Proteins: Struct., Funct., Genet. 5*, 183–201.
McCammon, J. A., & Harvey, S. C. (1987) *Dynamics of Proteins and Nucleic Acids*, Cambridge University Press, New York.
Meador, W. E., Means, A. R., & Quiocho, F. A. (1993) *Science 262*, 1718–21.
Qian, Y. Q., Otting, G., Tokunaga, F. K., Affolter, M., Gehering, W. J., & Wuthrich, K. (1992) *Proc. Natl. Acad. Sci. U.S.A. 89*, 10738–42.
Rasmussen, B. F., Stock, A. M., Ringe, D., & Petsko, G. A. (1992) *Nature 357*, 423–4.
Riddles, P. W., Blakeley, R. L., & Zerner, B. (1979) *Anal. Biochem. 94*, 75–81.
Rini, J. M., Schulze-Gahmen, U., & Wilson, I. A. (1992) *Science 255*, 959–65.
Schulz, G. E. (1991) *Curr. Opin. Struct. Biol. 1*, 883–8.
Shortle, D., & Meeker, A. K. (1986) *Proteins: Struct., Funct., Genet. 1*, 81–9.
Shortle, D., Meeker, A. K., & Freire, E. (1988) *Biochemistry 72*, 4761–8.
Stone, M. J., Fairbrother, W. J., Palmer, A. G. III., Reizer, J., Saier, M. H., Jr., & Wright, P. E. (1992) *Biochemistry 31*, 4394–406.
Stryer, L. (1978) *Annu. Rev. Biochem. 47*, 819–46.
Torchia, D. A., Sparks, S. W., & Bax, A. (1989) *Biochemistry 28*, 5509–24.
van der Goot, F. G., González-Manas, J. M., Lakey, J. H., & Pattus, F. (1991) *Nature 354*, 408–10.
Wu, P. G., & Brand, L. (1992) *Biochemistry 31*, 7939–47.
Wu, P. G., Rice, K. G., Brand, L., & Lee, Y. C. (1991) *Proc. Natl. Acad. Sci. U.S.A. 88*, 9355–9.